COMPUTER MODELING OF THE STALLED FLOW OF A ROTATING CYLINDER AND THE REVERSE MAGNUS EFFECT

S. M. Belotserkovskii, V. N. Kotovskii,
M. I. Nisht, and R. M. Fedorov

UDC 533.695.5

Unsteady stalled flow around a rotating cylinder is investigated in a numerical experiment. Attention is mostly given to the reverse Magnus effect which was discovered in tube experiments at some critical rotational speed of the cylinder.

Transverse flow around a rotating cylinder has been investigated by many authors, chiefly experimentally, for more than 200 years. A review of these investigations is given in [1]. They were carried out with different values of the relative rotational speed $\Theta = V_T/U_0$, different Reynolds numbers, degrees of turbulence of the incoming stream, degree of surface roughness, and other parameters.

It was established that the lift of the cylinder (Magnus effect) increases with its increasing rotational speed. However, it was found by recent experiments [1, 2] that in the range $0<\Theta\lesssim 0.5$ there may arise conditions of flow around a rotating cylinder such that the lift abruptly decreases, and with some combinations of the Reynolds numbers and Θ there may arise a "negative" Magnus effect (the lift changes sign).

For calculating nonsteady stalled flow around a rotating cylinder, we used in the present work an approach explained in [3]. It is based on the synthesis of the method of discrete vortices [4] and the theory of boundary layers.

The calculation scheme of flow is presented in Fig. 1. From the solution of the problem of nonviscous flow with vortex wakes [3] around a cylinder we determined the speed of the liquid relative to the cylinder surface taking the rotation of the cylinder into account

$$V_0 = U_{0l} + W_l + \frac{1}{2}(\gamma_\Sigma - \omega d).$$

Here W is the speed induced by the total adjoint vortices Γ_Σ of the cylinder and by the free vortices Δ of the vortex sheets. The subscript l denotes the tangential direction to the cylinder.

From the distribution of the speed V_0 on the cylinder surface we determined the position of the points of inflow H_1, H_2, ... (Fig. 1), i.e., the points at which the speed of the liquid in relative motion on the rotating cylinder is equal to zero. As in [1], these points were made identical with the starting points of the boundary layer. In the general case of a rotating cylinder they do not coincide with the critical points K_1, K_2, ..., at which the speed of absolute motion of the liquid is equal to zero. Since the boundary layer on the cylinder surface is relatively thin, we took it that the velocity of transport across its thickness is constant. The flow in the boundary layer was therefore calculated in relative motion. As boundary conditions for calculating the boundary layer we used the velocity distribution of the relative motion of a nonviscous liquid, and as its point of separation we took, as in [3], such a point on the cylinder surface at which $\partial u/\partial n \to 0$. The separating boundary layer was considered completely dislodged into the region of potential flow in the form of vortex sheets with an intensity equal to the vorticity of the boundary layer at the points of its separation [3].

In the process of interaction of the above-mentioned vortex sheets, zones of reverse flow may originate in the direct vicinity of the cylinder, with the formation not of one (frontal) but of several critical points and starting points of the boundary layer. Figure

Translated from Inzhenerno-Fizicheskii Zhurnal, Vol. 48, No. 2, pp. 244-250, February, 1985. Original article submitted November 24, 1983.

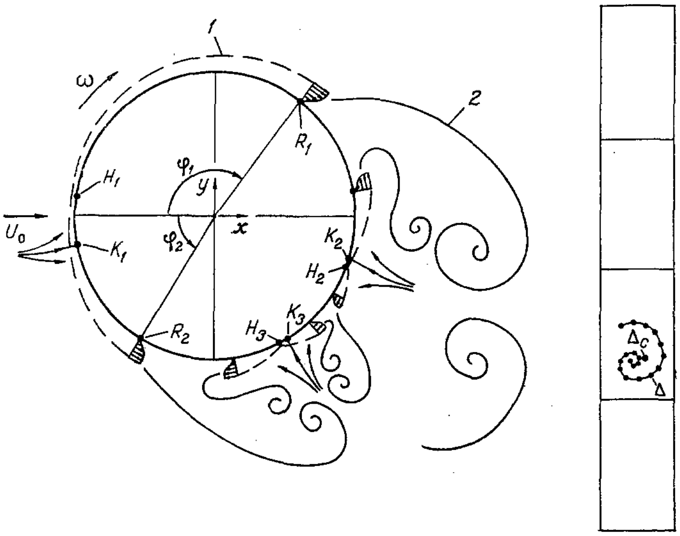

Fig. 1. Flow pattern: 1) boundary of the boundary layer; 2) free vortex sheet.

1 shows three such zones. In such cases the calculation of viscous flow in the boundary layer was carried out by starting from each point of inflow.

The flow parameters in the viscous range are determined by integrating the system of differential equations of the nonsteady boundary layer which, with the generally accepted notation, is written as follows:

$$\frac{\partial u}{\partial l}+\frac{\partial v}{\partial n}=0,\quad \frac{\partial u}{\partial t}+u\frac{\partial u}{\partial l}+v\frac{\partial u}{\partial n}=-\frac{1}{\rho}\frac{\partial p}{\partial l}+\frac{1}{\rho}\frac{\partial \tau}{\partial n}. \tag{1}$$

The boundary conditions used in solving the system (1) are usually the condition of adhesion of liquid particles to the cylinder surface and the tending of the longitudinal velocity in the boundary layer on its outer boundary toward the velocity of the outer flow, i.e.,

$$u=0,\ v=0 \text{ for } n=0;\ u\to V_0 \text{ for } n\to\delta.$$

In the general case of a turbulent boundary layer the shear stress τ is determined via the pulsation components of the velocity u' and v' by the expression

$$\tau=\mu\left(1-\frac{\overline{\rho u'v'}}{\mu\partial u/\partial n}\right)\frac{\partial u}{\partial n}=\mu(1+\varepsilon)\frac{\partial u}{\partial n},$$

and for a laminar boundary layer by Newton's formula

$$\tau=\mu\frac{\partial u}{\partial n}.$$

For closing the system of differential equations of a nonsteady turbulent boundary layer (1) we used a two-layer model of turbulent viscosity which may be written in the following form [5]:

$$\varepsilon=\begin{cases}\dfrac{1}{\nu}(\varkappa_1 n)^2\left[1-\exp\left(-\dfrac{n}{\varkappa_2\nu}\sqrt{\dfrac{\tau_w}{\rho}+\dfrac{dp}{dl}\dfrac{n}{\rho}}\right)\right]^2\times\\ \times\left|\dfrac{\partial u}{\partial n}\right|,\quad 0\leqslant n\leqslant n_0,\\ \dfrac{1}{\nu}\varkappa_3\dfrac{\dfrac{1}{V_0}\int\limits_0^\infty(V_0-u)\,dn}{1+\varkappa_4(n/\delta)^6},\quad n>n_0,\end{cases} \tag{2}$$

where $\varkappa$ are empirical constants ($\varkappa_1=0.41$; $\varkappa_2=26$; $\varkappa_3=0.0168$; $\varkappa_4=5.5$), and n_0 is the coordinate of the interlinking point of two layers of the boundary layer. It is chosen from the condition of continuity of the vortex viscosity across the boundary layer.

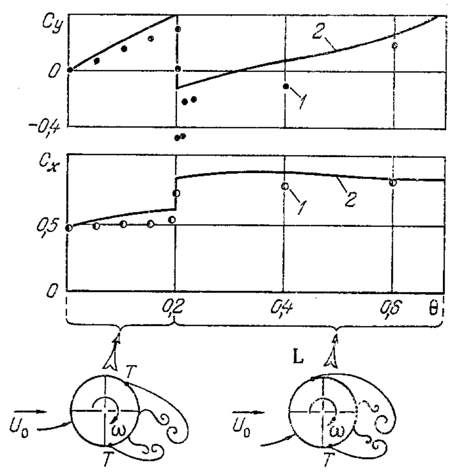

Fig. 2

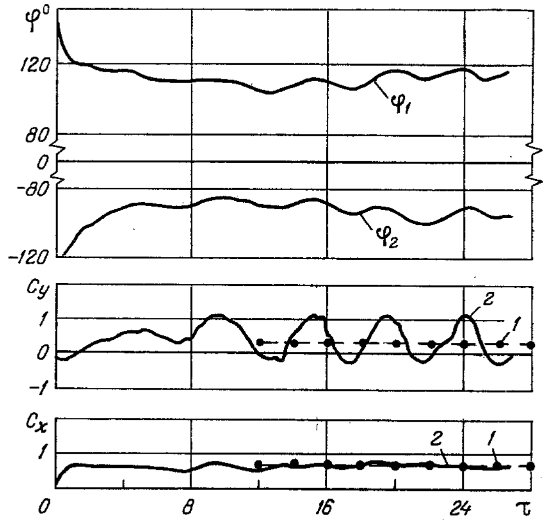

Fig. 3

Fig. 2. The effect of the relative rotational speed Θ on the lift coefficient C_y and the drag coefficient C_x (dimensionless magnitudes): 1) experimental data of [2]; 2) calculation.

Fig. 3. Peculiarities of the change of position of the points of separation φ_1 and φ_2 (deg), of the lift coefficient C_y and of the drag coefficient C_x in time τ for Θ = 0.2 (dimensionless magnitudes): 1) experimental data of [2]; 2) calculation.

The expression for turbulent viscosity (2) does not take the level of turbulence of the outer stream into account, but it can be taken into account, e.g., by a method explained in [6]. The system of differential equations (1) jointly with expression (2) for turbulent viscosity was integrated by the finite-difference method.

To economize on storage capacity of the computer and computer time expended on calculating nonviscous flow at each step, a number of discrete vortices were united when the bunch of vortices was sufficiently far from the cylinder, and this was done at each cell of the grid that was not less than 2-3 diameters behind the cylinder (Fig. 1). The circulation of a unifying discrete vortex was equal to the algebraic sum of the circulations of the discrete vortices in the given cell of the grid $\Delta_c = \sum_{i=1}^{\mu} \Delta_i$, and its coordinates were determined with a view to the magnitude of the circulation of the unified discrete vortices (μ is the number of unified vortices).

In calculating the nonsteady stalled flow around a motionless and an oscillating cylinder, Belotserkovskii et al. [7] established that, as in the experiment [8], the velocity of the longitudinal motion of vortex bunches is approximately 80% of the velocity of the incoming flow. The velocity of the unifying vortex was therefore henceforth adopted equal to $0.8 \cdot U_0$.

By special methodological investigations it was established that the results of the calculations do not differ by more than 2-3% from the results of calculations without the described unification, and the time needed for the calculation was reduced by approximately 40%.

Bychkov and Kovalenko [2] presented detailed experimental data on the coefficients C_y and C_x of a rotating cylinder with transverse flow around it and with different values of Θ and Re and a low degree of turbulence of the incoming flow. In Fig. 2 separate points indicate the experimental dependences of C_y and C_x on Θ with Re = $0.64 \cdot 10^6$. It can be seen that when Θ = 0.2, which in [2] was found to be critical, there occurs a jumplike change of the values of C_y and C_x; this indicates that there is an abrupt change in the flow regime. The authors of [1, 2] assumed that this effect is connected with transient phenomena in the boundary layer. With Reynolds numbers Re < Re_{cr} on that part of the front face of the rotating cylinder that moves against the flow, the laminar flow in the boundary layer, occurring with small $\Theta < \Theta_{cr}$, changes into turbulent flow at larger $\Theta > \Theta_{cr}$.

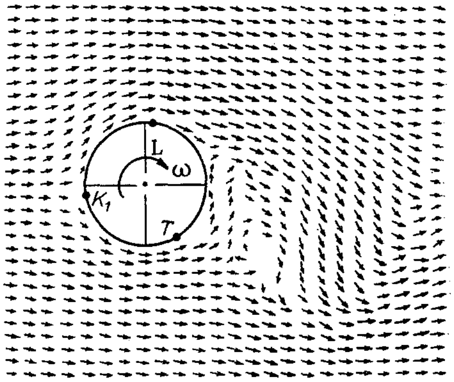

Fig. 4. Kinematic velocity field of a rotating cylinder.

It seems that on this part of the surface the number $Re_0 = V_0 d/\nu$, determined according to the local relative flow velocity, becomes larger than its critical value. Flow in the boundary layer is therefore turbulized, and the point of separation moves downstream. Because of the increased region of flow without separation on this surface, the lift acting on the rotating cylinder decreases to a negative value. On part of the surface moving in the direction of the outer flow, the flow in the boundary layer remains laminar.

With further increase of the parameter of rotation Θ, the points of separation of the boundary layer shift in the direction in which the cylinder rotates, and the lift continues to increase.

When $Re > Re_{cr}$ and the flow in the boundary layer of the front part of the cylinder is turbulent, the flow in the boundary layer becomes laminar when the parameter of rotation Θ increases because of the reduced relative velocity, and thus also of the local number Re_0 on the front face of the cylinder moving in the direction of the flow. This is the cause of the shift of the point of separation upstream, of the reduced size of the zone of flow without separation on this part of the surface, and of reduced lift.

Thus, the cause of the reverse of the lift of a rotating cylinder for $\Theta = \Theta_{cr}$ is the sudden shift of one of the points of separation of the boundary layer in the front part of the cylinder.

By using the above-explained flow pattern, we carried out systematic calculations of nonsteady stalled flow around a smooth rotating cylinder with different Reynolds numbers. Beginning from the value $\Theta \geqslant \Theta_{cr}$ with $Re < Re_{cr}$, on that part of the surface of the rotating cylinder that moves against the flow, the flow in the boundary layer was calculated as turbulent, and on the part of the surface moving in the direction of the flow as laminar.

With $Re > Re_{cr}$, in the range $\Theta \geqslant \Theta_{cr}$ the flow in the boundary layer on the part of the cylinder surface moving with the flow was calculated as laminar while turbulent flow was maintained on the surface moving against the flow. In the calculations we used the dependence $\Theta_{cr} = f(Re)$ obtained experimentally in [2].

In the rear part of the cylinder, because of the high level of turbulence of the outer flow in consequence of the strong interaction of the free vortex sheets, the flow in the boundary layer was considered to be turbulent.

Figure 3 presents the results of the calculation of nonsteady stalled flow around a rotating cylinder at the critical rotational speed $\Theta_{cr} = (1/2)\omega_{cr} d/U_0 = 0.2$ and Reynolds number $Re = 0.64 \cdot 10^6$, which is supercritical for a motionless cylinder. In the calculation under consideration it was therefore assumed that the flow in the boundary layer on the upper cylinder surface is still maintained turbulent. It can be seen from Fig. 3 that as with a motionless cylinder, after the passage of approximately 7-8 units of dimensionless time $\tau = U_0 t/d$, a periodic nature of flow with the aerodynamic Strouhal number ~0.2 becomes established.

An analysis of the calculations showed that in consequence of the rotation of the cylinder, the boundary layer on its upper surface is subjected to a relatively smaller longitudinal pressure gradient (especially in the region of elevated pressure) than on the lower surface. The result is that the boundary layer on the upper surface opens up further downstream than on the lower surface. Therefore, the mean value of the angle $\varphi_1=110°$, and $\varphi_2=-90°$, i.e., in comparison with a motionless cylinder the points of separation of the boundary layer are shifted in the direction of rotation of the cylinder.

The mean values of the lift and drag coefficients are in satisfactory agreement with the experimental data of [2]. Analogous calculations with the same Reynolds number were carried out in the range of values of relative rotational speeds $0\leqslant\Theta\leqslant0.8$. It can be seen from Fig. 2 that with increasing rotational speed, the lift coefficient of the cylinder increases practically linearly. When $\Theta = 0.2$, C_y abruptly decreases to negative values in consequence of the transition of the flow in the boundary layer on the upper surface from turbulent to laminar. When Θ increases further, C_y again increases in the range $\Theta>\Theta_{cr}$.

With increasing Θ, when $\Theta<\Theta_{cr}$, the drag coefficient of the cylinder increases only slightly. This is so because in this range of values of Θ the point of separation on the upper surface shifts less in the direction of rotation than on the lower surface. As a result, the zone of rarefaction somewhat increases on the bottom part of the cylinder, and this leads to an increase of its drag.

With values $\Theta=\Theta_{cr}$, in consequence of the change of the flow in the boundary layer from turbulent to laminar and the abrupt shift of the point of separation on the upper surface against the flow, the zone of rarefaction increases in the bottom region of the cylinder, and this leads to a jumplike increase of the drag.

An analysis of the results of the calculations showed that in the supercritical range of values of Θ the drag of the cylinder changes only slightly. This is so because on account of the mutual shift of the points of separation of the boundary layer on the upper and lower surface in the direction of rotation of the cylinder, the size of the zone of rarefaction in the bottom region of the cylinder remains approximately constant.

The formation of the boundary layer in the bottom region of the cylinder, its separation, and interaction with the boundary layer separating from the front part are analogous to the case of a motionless cylinder [3].

Calculations of nonsteady stalled flow around a rotating cylinder with other Reynolds numbers also showed qualitative and quantitative agreement with the experimental data.

Figure 4 shows the velocity field and the near aerodynamic wake behind a rotating cylinder with $Re = 0.64\cdot10^6$ and $\Theta = 0.75$. The figure also shows the time-averaged position of the critical point K, of the points of separation of the laminar (L) and of the turbulent (T) boundary layers with the upper and lower surface of the front part of the cylinder. It can be seen from the flow pattern that, as in the experiment, the flow curves in the vicinity of the rotating cylinder.

Thus, the mathematical model of nonsteady stalled flow around a rotating cylinder, suggested in the present article, makes it possible to determine the aerodynamic flow characteristics which agree qualitatively and quantitatively with the experimental data.

NOTATION

d, diameter of the cylinder; x, y, Cartesian coordinates; φ, angular position of the points of separation of the boundary layer; U_0, translational speed of the cylinder; V_τ, circumferential rotational speed of the cylinder; ω, angular rotational speed of the cylinder; W, velocity induced by vortices; u, v, longitudinal and transverse velocity, respectively, in the boundary layer in relative motion; γ_Σ, vorticity of the summary adjoint vortex layer; ν, kinematic viscosity; l, tangent to the cylinder surface; n, normal to the cylinder surface; δ, thickness of the boundary layer; C_y, lift coefficient; C_x, drag coefficient; $Re = U_0d/\nu$, Reynolds number; $\tau = U_0t/d$, dimensionless time; t, time; τ_w, surface friction; p, pressure; ρ, density; μ, dynamic viscosity; ε, dimensionless turbulent viscosity.

LITERATURE CITED

1. V. M. Svenson, "The Magnus effect: review of the results of an investigation," Tekh. Mekh., No. 3, 182-193 (1961).
2. N. M. Bychkov and V. M. Kovalenko, The Aerodynamic Characteristics of a Rotating and a Motionless Circular Cylinder in a Transverse Flow [in Russian], Siberian Branch, Academy of Sciences of the USSR, Institute of Theoretical and Applied Mechanics, Preprint No. 7 (1980).

3. S. M. Belotserkovskii, V. N. Kotovskii, M. I. Nisht, and R. M. Fedorov, "Mathematical modeling of nonsteady stalled flow around a circular cylinder," Izv. Akad. Nauk SSSR, Mekh. Zhidk. Gaza, No. 4, 138-146 (1983).
4. S. M. Belotserkovskii and M. I. Nisht, Stalled Flow and Flow without Separation of an Ideal Liquid around Thin Wings [in Russian], Nauka, Moscow (1978).
5. T. Cebeci, A. M. O. Smith, and G. Mosinskis, "Calculation of compressible adiabatic turbulent boundary layers," AIOO J., 8, No. 11, 1974-1982 (1970).
6. I. A. Belov, Models of Turbulence [in Russian], Leningrad Mechanical Institute (Leningradskii Mekhanicheskii Institut), Leningrad (1982).
7. S. M. Belotserkovskii, V. N. Kotovskii, M. I. Nisht, and R. M. Fedorov, "Computer study of the peculiarities of flow around an oscillating cylinder," Inzh.-Fiz. Zh., 47, No. 1, 41-47 (1984).
8. D. I. Blokhintsev, The Acoustics of Inhomogeneous Moving Media [in Russian], Nauka, Moscow (1981).

ANALYSIS OF THE DRAG OF TWO DISCS IN A TURBULENT INCOMPRESSIBLE FLUID FLOW

S. A. Isaev

UDC 532.517.4

The effect of reducing the drag of two discs is investigated by using difference modeling of their flow by using the two-parameter $k - \varepsilon$ turbulence model.

Analysis of the aerodynamic drag of two blunt bodies located behind each other in a uniform flow is represented by one of the urgent problems of the aerodynamics of poorly streamlined bodies. Its practical value is to the necessity of predicting the aerodynamic characteristics of systems of poorly streamlined bodies, on the one hand, and to the tendency to organize the flow around bodies of revolution by using the premeditated formation of developed circulation zones near their surface in order to improve their characteristics substantially [1], on the other. It is established in [1-3] that a significant diminution in the profile drag is observed in the axisymmetric flow around groups of bodies comprised of two discs, or a disc and a cylinder, as compared to the case of their isolated flow. Thus, by setting a disc of appropriate size at the optimal distance ahead of a single disc, a configuration can be obtained whose total drag would be 81% less than for a single disc, while the profile drag coefficient for a disc—cylinder composition can reach the value 0.02, i.e., close to the pressure drag coefficient in the case of potential flow around a body.

As follows from the papers mentioned above, interaction between the wake behind a disc with the large-diameter disc located downstream can be stable in nature; the flow configuration is determined greatly by the presence of such elements of different scale as the viscous shear layer and the circulation zones. The sharp edges of the discs turbulizing the stream for comparatively moderate Reynolds numbers (on the order of 10^3) result in a mode of developed turbulent flow around the discs, for which a sufficiently weak dependence of the body drag on the Reynolds number, in particular, is characteristic. The complexity of the flow occurring around the discs and the interrelation between the components of its structural elements suggest turning to numerical modeling of the flow around the discs on the basis of solving the Reynolds equations by finite-difference methods in combination with a semiempirical two-parameter turbulence model $k - \varepsilon$ consisting of the introduction of two differential equations for the turbulent energy fluctuations k and its dissipation velocity ε, a number of semiempirical constants, and an algebraic expression for the turbulent viscosity coefficient. It is considered that such a turbulence model correctly describes the developed turbulent flow mode.

The purpose of this paper is to compute the drag of a configuration of two discs of different size in the stationary uniform flow of an incompressible fluid in the ranges of varia-

---

Leningrad Mechanical Institute. Translated from Inzhenerno-Fizicheskii Zhurnal, Vol. 48, No. 2, pp. 251-256, February, 1985. Original article submitted December 27, 1983.

 0022-0841/85/4802-0180$09.50